



New phloroglucinol derivatives from the whole plant of *Hypericum uralum*



Xiaoqing Li, Yun Li, Jianguang Luo*, Zhongbo Zhou, Guimin Xue, Lingyi Kong*

Jiangsu Key Laboratory of Bioactive Natural Product Research, State Key Laboratory of Natural Medicines, China Pharmaceutical University, 24 Tong Jia Xiang, Nanjing 210009, People's Republic of China

ARTICLE INFO

Keywords:

Hypericum uralum

Guttiferae

Phloroglucinol derivatives

MDR reversal activity

ABSTRACT

Seven new phloroglucinol derivatives, uralones L–R (1–7), were isolated from the whole plant of *Hypericum uralum*. The structures of new compounds were unambiguously elucidated by comprehensive spectroscopic analysis, and the absolute configurations of the vic-diol groups were determined by $\text{Mo}_2(\text{OAc})_4$ -induced electronic circular dichroism experiments. Their capability to reversal the multidrug resistance in doxorubicin-induced resistant MCF-7/DOX sublines showed that compounds 1, 5, 6, 7 exerted a potential effect of doxorubicin susceptibility.

1. Introduction

Investigations of the constituents from the family Guttiferae have revealed a number of biologically and structurally interesting secondary metabolites, including naphthodianthrones, flavonoids, xanthenes, benzophenones, and phloroglucinol derivatives [1–5]. Among them, polycyclic polyprenylated acylphloroglucinols (PPAPs) are prominent characteristic metabolites, and feature a highly oxygenated and densely substituted skeleton decorated with prenyl or geranyl side chains [6]. Numerous literatures have been reported that PPAPs exhibit a broad spectrum of pharmacological activities, such as anti-neurodegenerative, antibacterial, anti-inflammatory, antioxidant, and anti-angiogenic activities [7–11]. *Hypericum uralum* Buch.-Ham. ex D. Don is distributed mainly in Tibet and northwest of Yunnan Province, P. R. China. The whole plant of *H. uralum* is used for antiphlogosis, detoxification and antipruritic in the Yunnan province [12]. In our previous study, a series of new PPAPs, uralones A–K, have been isolated from the petroleum ether extract of the whole plant of *H. uralum*, some of them showed significant protective effects against induced injury in PC12 cells [13]. As part of our ongoing search for bioactive PPAPs from natural sources, further investigations on *H. uralum* led to the isolation of seven new compounds, namely uralones L–R (1–7) (Fig. 1). Herein, we report the isolation, structural elucidation, and multidrug resistance (MDR) reversal activity of these isolates.

2. Experimental

2.1. General

Optical rotations were measured with a JASCO P-1020 polarimeter (Jasco, Tokyo, Japan). UV spectra were obtained on a UV-2450 UV/Vis spectrophotometer (Shimadzu, Tokyo, Japan). IR spectra (KBr disks, in cm^{-1}) were acquired using a Bruker Tensor 27 spectrometer (Bruker, Karlsruhe, Germany). A JASCO J-810 spectropolarimeter (Jasco, Tokyo, Japan) was used to record ECD spectra. NMR spectra were acquired in CDCl_3 at 303 K on Bruker Avance III NMR spectrometer (^1H NMR: 500 MHz or 600 MHz; ^{13}C NMR: 125 MHz or 150 MHz) with TMS as the internal standard. Chemical shifts (δ) and coupling constants (J) are expressed in parts per million (ppm) and hertz (Hz), respectively. ESIMS data were obtained using an Agilent 1100 Series LC/MSD Trap mass spectrometer, and HRESIMS data were collected using an Agilent 6520B UPLC-Q-TOF mass spectrometer (Agilent Technologies, Santa Clara, CA, USA). Silica gel (100–200 and 200–300 mesh; Qingdao Haiyang Chemical Co., Ltd., Qingdao, China), Sephadex LH-20 (40–70 μm ; Amersham Pharmacia Biotech AB, Uppsala, Sweden), and Fuji ODS RP- C_{18} (40–63 μm , Tokyo, Japan) were applied to column chromatography. TLC (GF_{254} , Qingdao Haiyang Chemical Co. Ltd., Qingdao, China) were used for monitoring fractions. Spots were visualized under UV light and by spraying the plates with a 1% vanillin-sulfuric acid solution, followed by heating. All solvents used were of analytical grade (Jiangsu Hanbang Sci. & Tech. Co., Ltd.). Preparative HPLC was performed on a Shimadzu LC-6AD Series instrument equipped with a Shim-pack RP- C_{18} column (20 mm \times 200 mm, i.d., 10 μm , Shimadzu, Tokyo, Japan) and 1100 Series Multiple Wavelength

* Corresponding authors.

E-mail addresses: luojg99@163.com (J. Luo), cpu_lykong@126.com (L. Kong).

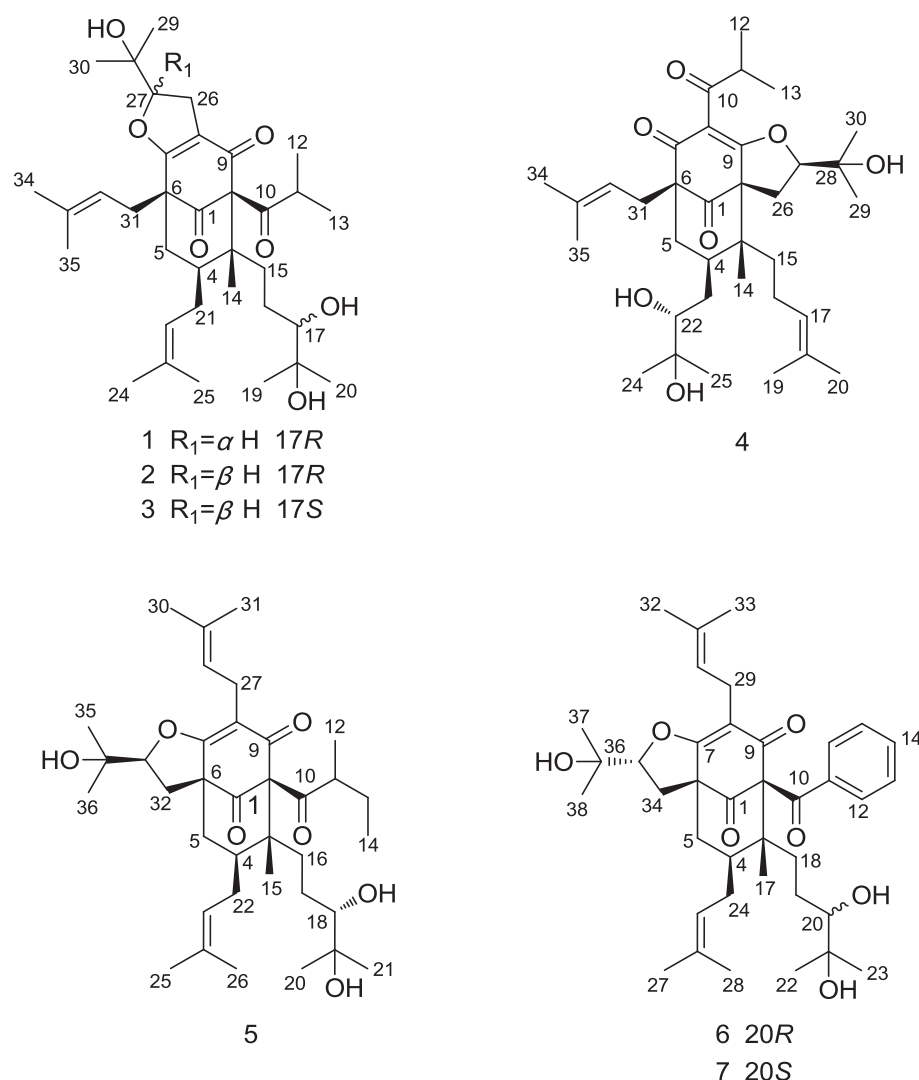


Fig. 1. Structures of compounds 1–7.

Detector. Recycling preparative HPLC was carried out on a Shimadzu LC-20A Series instrument equipped with a Shim-pack RP-C₁₈ column (20 mm × 200 mm, i.d., 5 μm, Shimadzu, Tokyo, Japan).

2.2. Plant material

The whole plants of *H. uralum* were collected in Yunnan Province, People's Republic of China, in June 2013 and were authenticated by Prof. Mian Zhang, School of Traditional Chinese Pharmacy, China Pharmaceutical University. Voucher specimens (2013-SEJST) were deposited at the Jiangsu Key Laboratory of Bioactive Natural Product Research, China Pharmaceutical University.

2.3. Extraction and isolation

The air-dried and powdered plant of *H. uralum* (10.0 kg) were extracted by refluxing with 95% aqueous EtOH (3 × 30 L), and then subsequently concentrated under reduced pressure. The obtained crude extract (1.3 kg) was suspended in H₂O (3 L), and partitioned successively with petroleum ether (3 × 3 L) and CH₂Cl₂ (3 × 3 L). The petroleum ether fraction (197 g) was loaded onto silica gel column chromatography (CC) and eluted with a gradient solvent system of petroleum ether-EtOAc (1:0 to 0:1) to yield five fractions (Fr. I–V). Fr. V (18 g) was subsequently chromatographed on a silica gel column using petroleum ether-EtOAc (3:1 to 0:1) as the eluent to obtain six fractions

(Fr. VA–VF). Fr. VE (2.1 g) was further separated to Sephadex LH-20 CC (CH₂Cl₂-MeOH, 1:1) to produce three fractions (Fr. VE1–VE3). Fr. VE3 (728 mg) was subjected to an ODS column using the isocratic system of 75% MeOH-H₂O to afford seven fractions (Fr. VE3a–VE3g). Fr. VE3d (86 mg) was then purified by preparative HPLC (MeOH-H₂O, 80:20), followed by recycling HPLC (MeCN-H₂O, 70:30) to yield compounds 1 (12.0 mg), 2 (7.0 mg), 3 (13.0 mg), and 4 (3.2 mg).

The CH₂Cl₂ fraction (106 g) was subjected to chromatography over MCI gel, eluted with a stepwise gradient of MeOH-H₂O (75% to 100%) to provide five fractions (Fr. A–E). Fr. A (29 g) was chromatographed onto a silica gel column, eluted with petroleum ether-EtOAc (10:1 to 0:1), to obtained six fractions (Fr. A1–A6). Fr. A3 (2 g) was separated on a Sephadex LH-20 CC (CH₂Cl₂-MeOH, 1:1) to yield six fractions (Fr. A3a–A3f). Fr. A3a (105 mg) was purified by preparative HPLC (MeOH-H₂O, 75:25), and then by recycling HPLC (MeCN-H₂O, 65:35) to yield compounds 5 (3.5 mg), 6 (4.5 mg) and 7 (10.0 mg).

2.4. Spectroscopic data

2.4.1. Uralione L (1)

Colorless oil; $[\alpha]_D^{25} - 29.0$ (c 0.1, MeOH); UV (MeOH) λ_{\max} (log ϵ) 204 (3.86), 282 (3.94) nm; CD (DMSO) λ_{\max} ($\Delta\epsilon$) 279 (+28.1), 302 (−32.7), 331 (+4.3) nm; IR (KBr) ν_{\max} 3433, 2974, 2929, 2875, 1726, 1614, 1447, 1408, 1382 cm^{−1}; ¹H NMR (CDCl₃, 500 MHz) and ¹³C NMR (CDCl₃, 125 MHz) data, see Tables 1 and 2; HRESIMS m/z

Table 1
¹H NMR data of compounds 1–7.

Position	1 ^a	2 ^a	3 ^a	4 ^a	5 ^b	6 ^a	7 ^a
4	1.67, m	1.60, m	1.70, m	1.60, m	1.61, m	1.84, m	1.86, m
5	1.95, dd (13.6, 4.3)	1.90, dd (13.6, 4.1)	1.90, dd (13.0, 4.0)	1.88, dd (13.5, 4.5)	2.04, m	2.14, m	2.12, m
	1.43, t (13.1)	1.45, t (13.3)	1.44, t (12.9)	1.42, t (13.5)	1.51, t (13.0)	1.63, overlapped	1.62, overlapped
11	2.09, m	2.17, m	2.15, m	2.50, m	1.73, m		
12	1.14, d (6.0)	1.11, d (6.5)	1.13, d (6.5)	1.15, d (6.5)	1.10, d (6.4)	7.43, d (7.4)	7.42, d (7.4)
13	1.04, d (6.0)	1.04, d (6.5)	1.04, d (6.5)	1.16, d (6.5)	1.67, m	7.22, t (7.8)	7.22, t (7.8)
					1.29, m		
14	1.04, s	1.04, s	1.04, s	1.11, s	0.77, t (7.4)	7.39, t (7.4)	7.39, t (7.4)
15	2.26, m	1.95, m	2.19, m	2.11, m	1.07, s	7.22, t (7.8)	7.22, t (7.8)
	1.75, m	1.74, m	1.74, m	1.62, m			
16	1.78, m	1.96, m	1.90, dd (13.0, 4.0)	2.17, m	2.04, m	7.43, d (7.4)	7.42, d (7.4)
	1.78, m	1.73, m	1.64, m	1.88, dd (13.5, 4.5)	1.93, m		
17	3.20, br d (9.5)	3.22, dd (10.0, 1.5)	3.20, br d (10.4)	4.99, t (6.4)	2.15, d (12.4)	1.20, s	1.20, s
18					3.25, d (10.0)	2.31, m	2.12, m
						1.84, m	1.30, m
19	1.19, s	1.18, s	1.19, s	1.67, s		2.14, m	2.12, m
						1.54, m	1.30, m
20	1.11, s	1.13, s	1.12, s	1.65, s	1.13, s	3.28, br d (9.8)	3.28, br d (9.8)
21	2.08, m	2.04, dd (14.3, 5.3)	2.05, dd (13.5, 5.2)	1.53, m	1.19, s		
	1.77, m	1.72, m	1.74, m	1.07, m			
22	4.94, t (6.7)	4.92, t (7.1)	4.91, t (6.5)	3.29, d (10.3)	2.15, m	1.15, s	1.14, s
					1.78, m		
23					4.93, t (7.0)	1.19, s	1.20, s
24	1.57, s	1.55, s	1.56, s	1.17, s		2.14, m	2.21, m
						1.54, m	1.86, m
25	1.70, s	1.67, s	1.67, s	1.13, s	1.70, s	4.99, t (7.5)	4.98, t (7.5)
26	2.97, d (9.2)	2.98, dd (15.0, 10.4)	2.99, dd (15.0, 10.5)	2.99, dd (10.5, 4.5)	1.57, s		
		2.89, dd (15.0, 7.8)	2.89, dd (15.0, 7.6)				
27	4.85, t (9.2)	4.74, dd (10.4, 7.8)	4.76, dd (10.4, 7.7)	4.80, t (10.5)	3.15, dd (14.4, 6.8)	1.72, s	1.72, s
					3.03, dd (14.3, 7.6)		
28					5.05, t (7.2)	1.60, s	1.60, s
29	1.18, s	1.23, s	1.24, s	1.25, s		3.14, dd (14.2, 6.5)	3.14, dd (14.2, 6.5)
						3.07, dd (14.2, 8.1)	3.07, dd (14.2, 8.1)
30	1.32, s	1.28, s	1.28, s	1.37, s	1.70, s	5.06, t (7.3)	5.05, t (7.3)
31	2.54, br d (15.0)	2.52, dd (14.6, 6.6)	2.53, dd (14.5, 6.4)	2.50, dd (13.0, 6.5)	1.65, s		
	2.47, dd (15.0, 9.0)	2.43, dd (14.6, 7.8)	2.43, dd (14.6, 7.9)	1.21, m			
32	4.98, br d (7.7)	5.05, t (7.1)	5.05, t (7.1)	4.99, t (6.4)	2.66, dd (12.9, 11.0)	1.67, s	1.67, s
					1.78, m		
33					4.57, dd (10.9, 5.6)	1.66, s	1.66, s
34	1.70, s	1.68, s	1.68, s	1.65, s		2.68, dd (13.2, 10.5)	2.70, dd (13.0, 10.5)
						1.84, m	1.86, m
35	1.69, s	1.67, s	1.67, s	1.58, s	1.22, s	4.64, dd (10.4, 6.0)	4.65, dd (10.4, 6.0)
36					1.40, s		
37						1.23, s	1.23, s
38						1.40, s	1.40, s

^a Data were recorded in CDCl₃ at 500 MHz.

^b Data were recorded in CDCl₃ at 600 MHz (δ in ppm, *J* in Hz).

609.3763 [M + Na]⁺ (calcd. for C₃₅H₅₄O₇Na, 609.3762).

2.4.2. Uralione M (2)

Colorless oil; [α]_D²⁵ + 28.6 (c 0.1, MeOH); UV (MeOH) λ_{\max} (log ϵ) 204 (3.90), 282 (3.97) nm; CD (DMSO) λ_{\max} ($\Delta\epsilon$) 279 (+ 35.8), 303 (− 32.1), 337 (+ 2.6) nm; IR (KBr) ν_{\max} 3434, 2973, 2930, 1726, 1618, 1448, 1408, 1381 cm^{−1}; ¹H NMR (CDCl₃, 500 MHz) and ¹³C NMR (CDCl₃, 125 MHz) data, see Tables 1 and 2; HRESIMS *m/z* 609.3761 [M + Na]⁺ (calcd. for C₃₅H₅₄O₇Na, 609.3762).

2.4.3. Uralione N (3)

Colorless oil; [α]_D²⁵ + 38.8 (c 0.1, MeOH); UV (MeOH) λ_{\max} (log ϵ) 204 (3.92), 282 (3.99) nm; CD (DMSO) λ_{\max} ($\Delta\epsilon$) 277 (+ 43.9), 303 (− 35.8), 335 (+ 3.5) nm; IR (KBr) ν_{\max} 3433, 2973, 2930, 2875, 1727, 1613, 1447, 1408, 1381 cm^{−1}; ¹H NMR (CDCl₃, 500 MHz) and ¹³C NMR (CDCl₃, 125 MHz) data, see Tables 1 and 2; HRESIMS *m/z* 609.3765 [M + Na]⁺ (calcd. for C₃₅H₅₄O₇Na, 609.3762).

2.4.4. Uralione O (4)

Colorless oil; [α]_D²⁵ + 91.4 (c 0.1, MeOH); UV (MeOH) λ_{\max} (log ϵ) 204 (3.81), 281 (3.83) nm; CD (DMSO) λ_{\max} ($\Delta\epsilon$) 279 (+ 71.5), 305

(− 29.9), 340 (+ 1.7) nm; IR (KBr) ν_{\max} 3435, 2973, 2929, 1724, 1615, 1446, 1383 cm^{−1}; ¹H NMR (CDCl₃, 500 MHz) and ¹³C NMR (CDCl₃, 125 MHz) data, see Tables 1 and 2; HRESIMS *m/z* 609.3759 [M + Na]⁺ (calcd. for C₃₅H₅₄O₇Na, 609.3762).

2.4.5. Uralione P (5)

Colorless oil; [α]_D²⁵ + 27.2 (c 0.1, MeOH); UV (MeOH) λ_{\max} (log ϵ) 203 (3.84), 272 (3.78) nm; CD (DMSO) λ_{\max} ($\Delta\epsilon$) 276 (+ 31.7), 302 (− 11.2), 334 (+ 3.6) nm; IR (KBr) ν_{\max} 3434, 2974, 2930, 1729, 1624, 1454, 1381 cm^{−1}; ¹H NMR (CDCl₃, 600 MHz) and ¹³C NMR (CDCl₃, 150 MHz) data, see Tables 1 and 2; HRESIMS *m/z* 623.3916 [M + Na]⁺ (calcd. for C₃₆H₅₆O₇Na, 623.2918).

2.4.6. Uralione Q (6)

Colorless oil; [α]_D²⁵ − 23.4 (c 0.1, MeOH); UV (MeOH) λ_{\max} (log ϵ) 203 (4.15), 247 (3.94), 273 (3.84) nm; CD (DMSO) λ_{\max} ($\Delta\epsilon$) 271 (− 51.5), 302 (+ 4.6) nm; IR (KBr) ν_{\max} 3435, 2974, 2927, 1727, 1695, 1622, 1448, 1382 cm^{−1}; ¹H NMR (CDCl₃, 500 MHz) and ¹³C NMR (CDCl₃, 125 MHz) data, see Tables 1 and 2; HRESIMS *m/z* 643.3606 [M + Na]⁺ (calcd. for C₃₈H₅₂O₇Na, 643.3605).

Table 2
¹³C NMR data of compounds 1–7.

Position	1 ^a	2 ^a	3 ^a	4 ^a	5 ^b	6 ^a	7 ^a
1	206.0	205.8	205.8	205.5	204.1	204.7	204.6
2	83.3	83.2	83.2	74.2	82.8	79.3	79.2
3	48.6	49.0	48.6	47.6	48.9	50.1	49.8
4	41.2	42.4	41.5	40.9	41.7	42.1	42.1
5	38.4	37.9	37.7	37.5	37.8	38.6	38.5
6	54.8	54.8	55.1	63.7	59.5	60.0	60.1
7	177.5	177.3	178.2	190.6	173.8	172.8	173.2
8	119.5	118.2	118.2	120.7	116.8	116.1	116.2
9	188.1	187.8	188.3	171.7	193.7	193.6	193.9
10	209.2	210.1	209.5	208.5	209.0	194.3	194.1
11	42.6	42.4	42.4	39.6	48.3	136.8	136.8
12	21.5	21.3	20.4	21.0	16.6	128.2	128.1
13	20.5	20.4	21.4	20.9	27.4	127.9	127.9
14	15.2	14.5	14.9	14.4	11.5	132.2	132.1
15	33.0	34.2	32.9	37.7	14.8	127.9	127.9
16	25.9	25.9	25.7	24.2	33.0	128.2	128.1
17	78.4	79.2	78.3	124.6	27.6	15.1	15.0
18	72.9	72.9	72.9	131.4	78.6	34.0	33.2
19	26.8	27.3	26.2	26.7	72.9	27.9	27.7
20	23.3	24.0	23.5	17.7	23.4	79.2	78.7
21	27.7	27.6	27.4	31.3	26.2	72.9	72.9
22	122.1	122.4	122.3	75.1	27.3	23.6	23.4
23	133.7	133.7	133.7	73.1	122.0	26.2	26.3
24	18.0	18.1	18.0	23.2	133.7	27.3	27.3
25	25.8	25.1	26.0	25.3	25.9	122.0	122.0
26	26.9	27.3	27.2	26.7	18.0	133.8	133.8
27	93.7	92.5	92.1	94.0	22.2	25.9	26.0
28	71.6	71.9	71.8	71.1	121.0	18.1	18.1
29	26.4	26.8	27.1	26.7	132.6	22.1	22.1
30	23.7	23.7	24.2	25.6	25.6	120.5	120.4
31	29.3	29.0	29.0	29.4	17.8	132.6	132.7
32	119.9	118.4	118.6	119.4	30.2	25.7	25.7
33	134.9	135.0	135.0	134.2	90.3	17.9	17.9
34	18.2	18.0	17.9	25.9	70.8	30.3	30.2
35	25.8	25.0	24.9	18.0	24.1	90.3	90.4
36					26.9	71.0	71.0
37						24.0	24.0
38						26.6	26.6

^a Data were recorded in CDCl₃ at 125 MHz.

^b Data were recorded in CDCl₃ at 150 MHz.

2.4.7. Uralione R (7)

Colorless oil; [α]_D²⁵ – 32.0 (c 0.1, MeOH); UV (MeOH) λ_{\max} (log ϵ) 203 (4.23), 247 (4.06), 274 (3.96) nm; CD (DMSO) λ_{\max} ($\Delta\epsilon$) 271 (– 89.6), 301 (+ 8.8), 337 (+ 1.6) nm; IR (KBr) ν_{\max} 3438, 2977, 2931, 1729, 1697, 1622, 1449, 1371 cm^{–1}; ¹H NMR (CDCl₃, 500 MHz) and ¹³C NMR (CDCl₃, 125 MHz) data, see Tables 1 and 2; HRESIMS m/z 643.3604 [M + Na]⁺ (calcd. for C₃₈H₅₂O₇Na, 643.3605).

2.5. Multidrug-resistance reversal assay

The MCF-7/DOX cells were cultured in RPMI 1640 containing 10% fetal bovine serum and antibiotics (100 U/mL of penicillin and 100 μ g/mL of streptomycin) at 37 °C in a 5% CO₂ incubator. After digested with trypsin, the cells suspension (5.0 \times 10³ cells/mL) were distributed evenly into 96-well culture plates and incubated for 24 h. A series of concentrations for the isolates in DMSO were added to each well. The optical density was measured at a test wavelength of 570 nm using a Universal Microplate Reader (Spectramax Plus 384, Molecular Devices, Sunnyvale, CA, USA) [14].

The MDR reversal assay, as previously reported [15], was performed at noncytotoxic concentration against multidrug resistant cells. MCF-7/DOX cells were distributed into 96-well culture plates at 5 \times 10³ cells/well. A full range of concentrations of DOX with or without samples or 10 μ M verapamil (positive control) were incubated with the cells. Then IC₅₀ values of DOX were calculated from plotted results using untreated cells as 100%. The reversal fold (RF) value, as a parameter of reversal potency, was calculated from dividing IC₅₀ of DOX alone by IC₅₀ of DOX

in the presence of test compounds with formula as following: reversal fold (RF) = IC₅₀ (MCF-7/DOX cells)/IC₅₀ (MCF-7/DOX cells combined with sample treatment). Each concentration was tested in three parallel wells.

3. Results and discussion

Uralione L (1) was obtained as colorless oil. It showed a pseudo-molecular ion peak at m/z [M + Na]⁺ 609.3763 in the HRESIMS spectrum, corresponding to a molecular formula of C₃₅H₅₄O₇ and indicating nine degrees of unsaturation. Its UV spectrum showed two absorption bands at 204 and 282 nm, which was coincided with the characteristic resonances for PPAPs [16]. The IR spectrum clearly implied the presence of a characteristic band for hydroxyl group at 3433 cm^{–1} and a sharp band for unconjugated carbonyl group at 1726 cm^{–1}. The ¹H NMR spectrum indicated the presence of two olefinic protons signals at δ_H 4.98 (1H, br d, J = 7.7 Hz) and 4.94 (1H, t, J = 6.7 Hz), nine singlet methyls and two doublet methyls at high-field resonance. The ¹³C NMR, with the help of HSQC, exhibited the signals for three carbonyl carbons (δ_C 209.2, 206.0, 188.1), six methylenes (δ_C 38.4, 33.0, 29.3, 27.7, 26.9, 25.9), two oxygen-bearing methines (δ_C 93.7, 78.4), and two methines (δ_C 42.6, 41.2). By analyzing the HSQC, HMBC, and ROESY spectra, all the proton and carbon signals (Tables 1 and 2, Fig. 2) were assigned unambiguously. The HMBC correlations from H-27 (δ_H 4.85) to the C-7 (δ_C 177.5), and C-8 (δ_C 119.4), from H-26 (δ_H 2.97) to the C-7 (δ_C 177.5), C-8 (δ_C 119.4), C-9 (δ_C 188.1), C-27 (δ_C 93.7), and C-28 (δ_C 71.6) confirmed that a dihydrofuran ring was formed between the C-7 enolic hydroxy group and the C-8 isoprenyl side chain. Furthermore, cross-peaks of H₂-31 to C-1 (δ_C 205.9), C-5 (δ_C 38.3), and C-6 (δ_C 54.7), of H₂-21 to C-4 (δ_C 41.2), and C-5 (δ_C 38.3) in HMBC spectrum, verified the location of two isoprenyl groups was at C-6, C-4, respectively. The abovementioned spectroscopic data of 1 revealed its structural features were similar to those of the known compound furohyperforin isomer 1 [17], except that the typical isoprenyl group at C-15 was replaced by a 3-methyl-2, 3-pentanedio moiety in compound 1. This was further evidenced by the HMBC correlations from H₂-16 (δ_H 1.78) to C-3 (δ_C 48.6), C-17 (δ_C 78.4), and from H-17 (δ_H 3.20) to C-15 (δ_C 33.0) in 1.

The relative configuration of 1 was determined by ROESY experiment, conjugated with the comparative analysis of the NMR data with its analogues. The chemical shift of C-4 (δ_C 41.2) and the chemical shift difference between H-5 β and H-5 α ($\Delta\delta_H$ ca. 0.52 ppm) suggested that the configuration of H-4 was in α -orientation [18]. The ROESY correlations of Me-14 (δ_H 1.04)/H-11 (δ_H 2.09), Me-14 (δ_H 1.04)/H-5 β (δ_H 1.43), and H-5 β (δ_H 1.43)/H-31 (δ_H 2.54), suggested that 1 possessed similar relative configuration at C-2, C-3, and C-6 with those of furohyperforin isomer 1. In addition, the diagnostic ROESY cross-peak of Me-30 (δ_H 1.32)/H-32 (δ_H 4.98) indicated that H-27 was α -oriented [19] (Fig. 2). In order to determine the absolute configuration of the

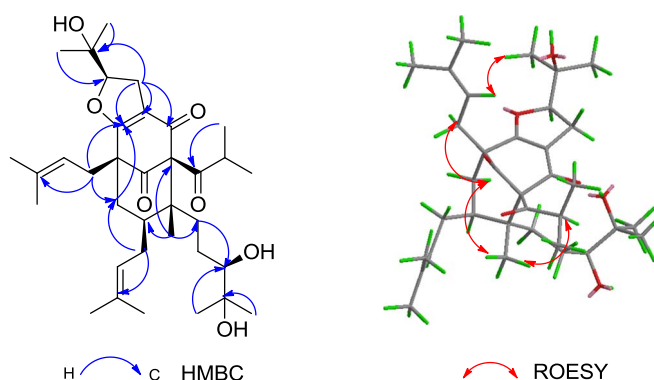


Fig. 2. Selected key HMBC and ROESY correlations of compound 1.

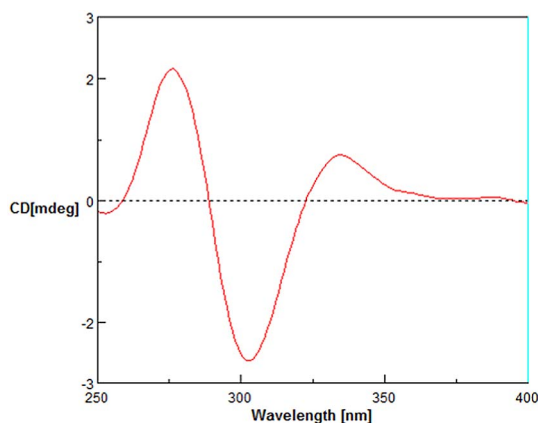


Fig. 3. $\text{Mo}_2(\text{OAc})_4$ -induced ECD spectrum of **1** in DMSO.

acyclic 17, 18-diol moiety in **1**, the Sneath's method [20,21], an induced ECD spectrum of in situ complexation with $\text{Mo}_2(\text{OAc})_4$ in DMSO solution was applied, in which the sign of the characteristic band at about 310 nm implied the absolute configuration of the chiral centers in the 1, 2-diol moiety [22,23]. Compound **1** showed a negative E band at 303 nm correlating with a 17R configuration (Fig. 3). Thus the structure of compound **1** was elucidated as shown in Fig. 1.

Uralones M (**2**) and N (**3**) were both isolated as colorless oil. Their molecular formula $\text{C}_{35}\text{H}_{54}\text{O}_7$ (nine double bond equivalents), were accommodated collectively by its HRESIMS sodium adduct ion (m/z 609.3761 in **2**; m/z 609.3765 in **3**) and ^{13}C NMR spectral data. Extensive analysis of their 1D and 2D NMR spectra, the planar structures as well as the stereogenic centers at C-2, C-3, C-4, and C-6 of compounds **2** and **3** were set up as those of compound **1**. Contrary to **1**, no ROESY cross-peak of Me-30/H-32 could be observed in compounds **2** and **3** [19]. However, H-27 showed cross-peaks with Me-29 and Me-30 [24], suggesting that the H-27 should be β -oriented. The reported data indicated that the orientation of hydroxypropyl at C-27 resulted in the slight difference of chemical shifts for both proton and carbon at this position. The 27 β -hydroxypropyl epimer always exhibited chemical shifts at a lower field compared to those of the corresponding 27 α -hydroxypropyl epimer [16,17,25–28]. It was found that the $\delta_{\text{C/H}}$ for C-27 of **2** and **3** ($\delta_{\text{C/H}}$ 4.74/92.5 in **2**; 4.76/92.1 in **3**) were at a higher field than those of **1** ($\delta_{\text{C/H}}$ 4.85/93.7) and this allowed us to confirm the 27 α -hydroxypropyl configurations for **2** and **3**. Furthermore, the complex-induced ECD spectrum of compound **2** exhibited a negative E band, indicating the 17R configuration, while compound **3** showed a positive E band, coinciding with the 17S configuration (Fig. 4). Thus the structures of **2** and **3** were established as depicted in Fig. 1.

Uralione O (**4**), obtained as a colorless oil, was determined to have a molecular formula $\text{C}_{35}\text{H}_{54}\text{O}_7$, by its HRESIMS (m/z 609.3759 [M

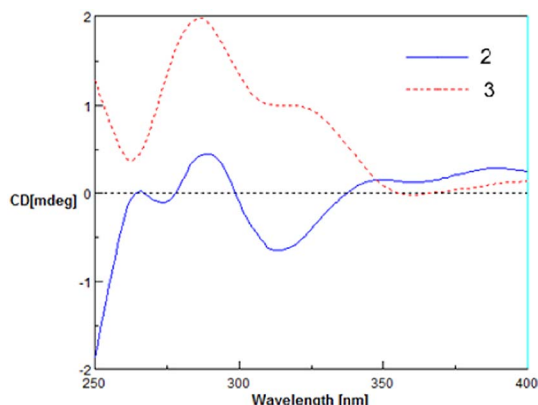


Fig. 4. $\text{Mo}_2(\text{OAc})_4$ -induced ECD spectra of compounds **2** and **3** in DMSO.

+ Na] $^+$) and NMR data, requiring nine double bond equivalents. The ^1H NMR spectrum of **4** revealed the presence of two isoprenyl groups (δ_{H} 4.99, 2H, t, J = 6.4 Hz), a 2-methylpropionyl moiety [δ_{H} 2.50 (1H, m), δ_{H} 1.15 (3H, d, J = 6.5 Hz), δ_{H} 1.16 (3H, d, J = 6.5 Hz)], a 3-methyl-2, 3-pentanediol moiety [δ_{H} 3.29 (1H, d, J = 10.3 Hz), δ_{H} 1.17 (3H, s), δ_{H} 1.13 (3H, s)], an oxidized 2, 2-dimethyl-2H-dihydrofuran ring [δ_{H} 2.99 (2H, dd, J = 10.5, 4.5 Hz), δ_{H} 4.80 (1H, t, J = 10.5 Hz), δ_{H} 1.37 (3H, s), δ_{H} 1.25 (3H, s)]. These observations indicated that compound **4** was structural similarity to those for attenuatumione E [29]. The significantly difference involving the typical isoprenyl group signals at C-4 was replaced by a set of 3-methyl-2, 3-pentanediol moiety signals in **4**, which was supported by the HMBC correlations from H-21 (δ_{H} 1.53) to C-4 (δ_{C} 40.9), C-3 (δ_{C} 47.6) and C-22 (δ_{C} 75.1), from H-5 (δ_{H} 1.88) and H-14 (δ_{H} 1.11) to C-4 (δ_{C} 40.9), from H-4 (δ_{H} 1.60) to C-3 (δ_{C} 47.6). The ROESY cross-peak of H-27 (δ_{H} 4.80) with H-15 (δ_{H} 2.11) indicated that H-27 was α -oriented (Fig. S4-9). The in situ $\text{Mo}_2(\text{OAc})_4$ complex-induced ECD spectrum of **4** exhibited a negative E band at about 310 nm, indicating a 17R configuration (Fig. S0). Therefore, the structure of **4** was assigned as shown in Fig. 1.

Uralione P (**5**) was isolated as a colorless oil. The observed pseudomolecular ion at m/z 623.3916 [M + Na] $^+$ in the HRESIMS spectrum and ^{13}C NMR data gave a molecular formula of $\text{C}_{36}\text{H}_{56}\text{O}_7$, indicating nine degrees of unsaturation. Comparison the ^1H NMR and ^{13}C NMR data with those of furoadhyperforin [17], revealed that they differed from the appearance of an oxygenated methine proton (δ_{H} 3.25, 1H, d, J = 10.0 Hz) and two oxygenated carbons (δ_{C} 78.6 and δ_{C} 72.9) in compound **5**. The key HMBC correlations from H-16 to C-2 (δ_{C} 82.8), C-3 (δ_{C} 48.9), C-4 (δ_{C} 41.7), C-15 (δ_{C} 14.8), C-17 (δ_{C} 27.6), and C-18 (δ_{C} 78.6), from H-18 to C-16 (δ_{C} 33.0), C-17 (δ_{C} 27.6), and C-19 (δ_{C} 72.9) indicated that the 3-methyl-2, 3-pentanediol moiety was located at C-3. ROESY cross-peaks of H-5 β /H-15 and Me-35/H-5 β indicated that H-33 was in α -orientation (Fig. S5-9). The in situ $\text{Mo}_2(\text{OAc})_4$ complex-induced ECD spectrum of **5** exhibited a positive E band, consistent with a 18S configuration (Fig. S0). Therefore, the structure of **5** was depicted as shown in Fig. 1.

Uraliones Q (**6**) and R (**7**) were both acquired as colorless oil. Based on the sodium adduct ion (m/z 643.3606 in **6**; m/z 643.3604 in **7**) and ^{13}C NMR data, establishing the molecular formula of **6** and **7** as $\text{C}_{38}\text{H}_{52}\text{O}_7$ with thirteen indices of hydrogen deficiency. The 1D and 2D NMR data of compounds **6** and **7** closely resembled with those of uralione E [13], the only difference lay in that the isoprenyl group at C-18 was oxidized to a 3-methyl-2, 3-pentanediol moiety. Comprehensive analysis of the ROESY spectrum indicated that compounds **6** and **7** possessed the β -orientation configuration of H-35 on the basis of the correlations of H-17/H-5 β , H-35/H-5 β . The 20R configuration in **6** was determined by the induced negative cotton effect, while the positive cotton effect of **7** suggested the 20S configuration in **7** (Fig. S0). Thus the structures of **6** and **7** were deduced as shown in Fig. 1.

Compounds **1–7** were other new PPAPs from the whole plant of *H. uralum*. From a biosynthetic perspective, polyprenylated acylphloroglucinols are considered to be produced by prenylation of acylphloroglucinols, which was formed by condensation of one acyl-CoA and three malonyl-CoA units, and subsequently by intramolecular cyclization [6]. The biogenetic starter can be an acyl group or a benzoyl group, both of them are found in the *Hypericum* species [29,31,34]. Compounds **1–5**, with an alkyl starter, maybe derived from leucine or isoleucine [7], while compounds **6** and **7**, with an aromatic starter, maybe derived from phenylalanine [35]. Although many studies on the biosynthesis of PPAPs have been reported, the precursor requires more in-depth research works.

Many phloroglucinol derivatives have been reported to possess moderate to significant cytotoxic activities against different cancer cell lines [30,31], as well as MDR cancer cell line [32,33]. Compounds **1–7** were investigated for their reversal activity towards multidrug resistance in available MCF-7/DOX cancer cells. Among them, compounds **2–4** exhibited inhibition rate less than 50% at the tested

Table 3
MDR reversal effects of the isolates on MCF-7/DOX cells.

Sample	IC ₅₀ (μM)	RF value
1 (10 μM)	7.72 ± 1.10	4.8
5 (30 μM)	7.48 ± 1.25	4.9
6 (30 μM)	2.32 ± 0.67	16.0
7 (30 μM)	5.61 ± 0.64	6.6
DOX	37.14 ± 3.73	1.0
Ver (10 μM)	1.17 ± 0.12	31.7

Verapamil was used as the positive control at 10 μM.

concentration of 50.0 μM and was considered to be inactive. As shown in Table 3, compounds 5, 6, and 7 exerted reversal activity of doxorubicin susceptibility at the tested concentration of 30 μM [Reverse fold (RF): 4.9, 16.0, 6.6-fold, respectively], as compared with the positive control, verapamil (10 μM, RF = 31.7). Compound 1 displayed moderate cytotoxicity against MCF-7/DOX cell at 30 μM, allowing us to assay its reversal effect at the lower concentration of 10.0 μM (RF = 4.8). These results further support the potential of this family of compounds for overcoming MDR in cancer therapy.

Conflict of interest

The authors declare no competing financial interests.

Acknowledgments

The work was supported by the National Natural Sciences Foundation of China (Program 81430092), the project funded by the Priority Academic Program Development of Jiangsu Higher Education Institutions (PAPD), and the Program for Changjiang Scholars and Innovative Research Team in University (IRT_15R63).

Appendix A. Supplementary data

The original HRESIMS, UV, IR, 1D NMR, 2D NMR, and ECD spectra for compounds 4–7 are available as Supporting Information. Supplementary data to this article can be found online at <https://doi.org/10.1016/j.fitote.2017.09.020>.

References

- [1] P. Avato, A survey on the *hypericum* genus: secondary metabolites and bioactivity, *Stud. Nat. Prod. Chem.* 30 (2005) 603–634.
- [2] J. Barnes, L.A. Anderson, J.D. Phillipson, St John's wort (*Hypericum perforatum* L.): a review of its chemistry, pharmacology and clinical properties, *J. Pharm. Pharmacol.* 53 (2001) 583–600.
- [3] A. Nahrstedt, V. Butterweck, Biologically active and other chemical constituents of the herb of *Hypericum perforatum* L. *Pharmacopsychiatry* 30 (1997) 129–134.
- [4] G. Rath, O. Potterat, S. Mavi, K. Hostettmann, Xanthones from *Hypericum roeperianum*, *Phytochemistry* 43 (1996) 513–520.
- [5] L.H. Hu, K.Y. Sim, Sampsoniones C-H, a unique family of polyphenylated benzophenone derivatives with the novel tetracyclo [7.3.1.1^{3,11}.0^{3,7}] teradecane-2,12,14-trione skeleton, from *Hypericum sampsonii* (Guttiferae), *Tetrahedron Lett.* 40 (1999) 759–762.
- [6] R. Ciochina, R.B. Grossman, Polycyclic polyphenylated acylphloroglucinols, *Chem. Rev.* 106 (2006) 3963–3986.
- [7] L. Verotta, Are acylphloroglucinols lead structures for the treatment of degenerative diseases, *Phytochem. Rev.* 1 (2002) 389–407.
- [8] W.K.P. Shiu, M.M. Rahman, J. Curry, P. Stapleton, M. Zloh, J.P. Malkinson, S. Gibbons, Antibacterial acylphloroglucinols from *Hypericum olympicum*, *J. Nat. Prod.* 75 (2012) 336–343.
- [9] C.M. Schempp, B. Winghofer, R. Ludtke, B.S. Haarhaus, E. Schopf, J.C. Simon, Topical application of St John's wort (*Hypericum perforatum* L.) and of its metabolite hyperforin inhibits the allostimulatory capacity of epidermal cells, *Brit. J. Dermatol.* 142 (2000) 979–984.
- [10] D. Schwarz, P. Kisselev, I. Roots, St John's Wort extracts and some of their constituents potentially inhibit ultimate carcinogen formation from benzo [a] pyrene-7, 8-dihydrodiol by human CYP1A1, *Cancer Res.* 63 (2003) 8062–8068.
- [11] B.M. Poveda, A.R. Quesada, M.A. Medina, Hyperforin, a bio-active compound of St John's Wort, is a new inhibitor of angiogenesis targeting several key steps of the process, *Int. J. Cancer* 117 (2005) 775–780.
- [12] Y.H. Li, Z.Y. Wu (Ed.), *In Flora of China*, 50 Science Press, Beijing, China, 1990, p. 27.
- [13] Z.B. Zhou, Z.R. Li, X.B. Wang, J.G. Luo, L.Y. Kong, Polycyclic polyphenylated derivatives from *Hypericum uratum*: neuroprotective effects and antidepressant-like activity of Uralodin A, *J. Nat. Prod.* 79 (2016) 1231–1240.
- [14] L. Yang, D.D. Wei, Z. Chen, J.S. Wang, L.Y. Kong, Reversal of multidrug resistance in human breast cancer cells by *Curcuma wenyuyin* and *Chrysanthemum indicum*, *Phytomedicine* 18 (2011) 710–718.
- [15] Y.L. Zhang, X.W. Zhou, L. Wu, X.B. Wang, M.H. Yang, J. Luo, J.G. Luo, L.Y. Kong, Isolation, structure elucidation, and absolute configuration of syncarpic acid-conjugated terpenoids from *Rhodomyrtus tomentosa*, *J. Nat. Prod.* 80 (2017) 989–998.
- [16] W.J. Xu, M.D. Zhu, X.B. Wang, M.H. Yang, J. Luo, L.Y. Kong, Hypermongones A-J, rare methylated polycyclic polyphenylated acylphloroglucinols from the flowers of *Hypericum monogynum*, *J. Nat. Prod.* 78 (2015) 1093–1100.
- [17] J.Y. Lee, R.K. Duke, V.H. Tran, J.M. Hook, C.C. Duke, Hyperforin and its analogues inhibit CYP3A4 enzyme activity, *Phytochemistry* 67 (2006) 2550–2560.
- [18] W. Gao, J.W. Hu, F. Xu, C.J. Wei, M.J. Shi, J. Zhao, J. Wang, B. Zhen, T.F. Ji, J.G. Xing, Z.Y. Gu, F. Xu, Polyisoprenylated benzoylphloroglucinol derivatives from *Hypericum scabrum*, *Fitoterapia* 115 (2016) 128–134.
- [19] X.Q. Chen, Y. Li, X. Cheng, K. Wang, J. He, Z.H. Pan, M.M. Li, L.Y. Peng, G. Xu, Q.S. Zhao, Polycyclic polyphenylated acylphloroglucinols and chromone O-glucosides from *Hypericum henryi* sub sp. uraloide, *Chem. Biodivers.* 7 (2010) 196–204.
- [20] G. Snatzke, U. Wagner, H.P. Wolff, Circular dichroism-LXXV 1: Cottonogenic derivatives of chiral bidentate ligands with the complex [Mo₂(OCCH₃)₄], *Tetrahedron* 37 (1981) 349–361.
- [21] L.D. Bari, G. Pescitelli, C. Pratelli, D. Pini, P. Salvadori, Determination of absolute configuration of acyclic 1, 2-diols with Mo₂(OAc)₄.1. snatzke's method revisited, *J. Organomet. Chem.* 66 (2001) 4819–4825.
- [22] T.X. Li, M.H. Yang, X.B. Wang, Y. Wang, L.Y. Kong, Synergistic antifungal meroterpenes and dioxolanone derivatives from the endophytic fungus *Guignardia* sp., *J. Nat. Prod.* 78 (2015) 2511–2520.
- [23] H. Yin, J.G. Luo, L.Y. Kong, Tetracyclic diterpenoids with isomerized isospongian skeleton and labdane diterpenoids from the fruits of *Amomum kravanh*, *J. Nat. Prod.* 76 (2013) 237–242.
- [24] R.D. Liu, Y.L. Su, J.B. Yang, A.G. Wang, Polyphenylated acylphloroglucinols from *Hypericum scabrum*, *Phytochemistry* 142 (2017) 38–50.
- [25] C. Hashida, N. Tanaka, Y. Kashiwada, M. Ogawa, Y. Takaishi, Prenylated phloroglucinol derivatives from *Hypericum perforatum* var. *angustifolium*, *Chem. Pharm. Bull.* 56 (2008) 1164–1167.
- [26] M. Matsuhisa, Y. Shikishima, Y. Takaishi, G. Honda, M. Ito, Y. Takeda, H. Shibata, T. Higuti, O.K. Kodzhimatov, O. Ashurmetov, Benzoylphloroglucinol derivatives from *Hypericum scabrum*, *J. Nat. Prod.* 65 (2002) 290–294.
- [27] J.R. Weng, C.N. Lin, L.T. Tsao, J.P. Wang, Terpenoids with a new skeleton and novel triterpenoids with anti-inflammatory effects from *Garcinia subelliptica*, *Chem. Eur. J.* 9 (2003) 5520–5527.
- [28] Y. Gao, N. Zhang, C.M. Chen, J.F. Huang, X.N. Li, J.J. Liu, H.C. Zhu, Q.Y. Tong, J.W. Zhang, Z.W. Luo, Y.B. Xue, Y.H. Zhang, Tricyclic polyphenylated acylphloroglucinols from St John's Wort, *Hypericum perforatum*, *J. Nat. Prod.* 80 (2017) 1493–1504.
- [29] Z.B. Zhou, Y.M. Zhang, K. Pan, J.G. Luo, L.Y. Kong, Cytotoxic polycyclic polyphenylated acylphloroglucinols from *Hypericum attenuatum*, *Fitoterapia* 95 (2014) 1–7.
- [30] L.H. Hu, K.Y. Sim, Cytotoxic polyphenylated benzoylphloroglucinol derivatives with an unusual adamantyl skeleton from *Hypericum sampsonii* (Guttiferae), *Org. Lett.* 1 (1999) 879–882.
- [31] X. Liu, X.W. Yang, C.Q. Chen, C.Y. Wu, J.J. Zhang, J.Z. Ma, H. Wang, L.X. Yang, G. Xu, Bioactive polyphenylated acylphloroglucinol derivatives from *Hypericum cohaerens*, *J. Nat. Prod.* 76 (2013) 1612–1618.
- [32] W. Hashida, N. Tanaka, Y. Kashiwada, M. Sekiya, Y. Ikeshiro, Y. Takaishi, Tomoeones A-H, cytotoxic phloroglucinol derivatives from *Hypericum ascyron*, *Phytochemistry* 69 (2008) 2225–2230.
- [33] N. Tanaka, Y. Kashiwada, M. Sekiya, Y. Ikeshiro, Y. Takaishi, Takaneones A-C, prenylated butylphloroglucinol derivatives from *Hypericum sikokumontanum*, *Tetrahedron Lett.* 49 (2008) 2799–2803.
- [34] W. Gao, W.Z. Hou, J. Zhao, F. Xu, L. Li, F. Xu, H. Sun, J.G. Xing, Y. Peng, X.L. Wang, T.F. Ji, Z.Y. Gu, Polycyclic polyphenylated acylphloroglucinol congeners from *Hypericum scabrum*, *J. Nat. Prod.* 79 (2016) 1538–1547.
- [35] S.B. Wu, C.L. Long, E.J. Kennelly, Structural diversity and bioactivities of natural benzophenones, *Nat. Prod. Rep.* 31 (9) (2014) 1158–1174.